Molecular Pharmacology Fast Forward. Published on January 30, 2014 as doi:10.1124/mol.113.090076

Title Page

Nanomolar Bifenthrin Alters Synchronous Ca^{2+} Oscillations And Cortical Neuron Development Independent of Sodium Channel Activity

Zhengyu Cao, Yanjun Cui, Hai M. Nguyen, David Paul Jenkins, Heike Wulff, and Isaac N. Pessah

Department of Molecular Biosciences, School of Veterinary Medicine, UC Davis, Davis CA 95616 U.S.A. (Z.C., Y.C., I.N.P.); Department of Pharmacology, School of Medicine, UC Davis, Davis, CA 95616 USA (H.M.N., D.P.J., H.W.)

Molecular Pharmacology Fast Forward. Published on January 30, 2014 as DOI: 10.1124/mol.113.090076
This article has not been copyedited and formatted. The final version may differ from this version.
MOL #90076

Running Title Page

Bifenthrin alters Ca^{2+} oscillations and neuronal development

Corresponding Author:

Isaac N. Pessah, Ph.D.

Department of Molecular Biosciences

School of Veterinary Medicine

1089 Veterinary Medicine Drive

University of California, Davis

Davis, CA 95616

E-mail: inpessah@ucdavis.edu

Tel: 530-752-6696

FAX: 530-752-4698

Number of:

Text Pages (29)

Tables (0)

Figures (8)

References (46)

Number of words:

Abstract (239)

Introduction (831)

Discussion (1283)

Abbreviations

CERB, cAMP response element-binding protein; DIV, days in vitro; E_{rest}, resting membrane potential; FLIPR, Fluorescence Imaging Plate Reader; GABA, gammãaminobutyric acid; MEA, multielectrode array; NDL PCB, non-dioxin like polychlorinated biphenyls; SCO, spontaneous Ca^{2+} oscillations; VGSC, voltage gated sodium channel

Molecular Pharmacology Fast Forward. Published on January 30, 2014 as DOI: 10.1124/mol.113.090076
This article has not been copyedited and formatted. The final version may differ from this version.
MOL #90076

Abstract

Bifenthrin, a relatively stable type I pyrethroid that causes tremors and impairs motor activity in rodents, is broadly used. Whether nanomolar bifenthrin alters synchronous Ca^{2+} oscillations (SCO) necessary for activity dependent dendritic development was investigated. Primary mouse cortical neurons were cultured 8-9 days *in vitro* (DIV), loaded with the Ca^{2+} indicator Fluo-4, and imaged using FLIPR Tetra. Acute exposure to bifenthrin rapidly increased the frequency of SCO 2.7-fold (EC_{50}=58nM) and decreased SCO amplitude by 36%. Changes in SCO properties were independent of modifications in voltage-gated sodium channels since 100nM bifenthrin had no effect on the whole-cell Na^+ current, nor influenced neuronal E_{rest}. The L-type Ca^{2+} channel blocker nifedipine failed to ameliorate bifenthrin-triggered SCO activity. By contrast, the mGluR 5 antagonist MPEP normalized bifenthrin-triggered increase in SCO frequency without altering baseline SCO activity, indicating that bifenthrin amplifies mGluR 5 signaling independent of Na^+ channel modification. Competitive (AP-5) and non-competitive (MK801) NMDAR antagonists partially decreased both basal and bifenthrin-triggered SCO frequency increase. Bifenthrin-modified SCO rapidly enhanced the phosphorylation of cAMP response element-binding protein (CREB). Sub-acute (48h) exposure to bifenthrin commencing 2 DIV enhanced neurite outgrowth and persistently increased SCO frequency and reduced SCO amplitude. Bifenthrin-stimulated neurite outgrowth and CREB phosphorylation were dependent on mGluR 5 activity since MPEP normalized both responses. Collectively these data identify a new mechanism by which bifenthrin potently alters Ca^{2+} dynamics and Ca^{2+}-dependent signaling in cortical neurons that have long term impacts on activity driven neuronal plasticity.

Molecular Pharmacology Fast Forward. Published on January 30, 2014 as DOI: 10.1124/mol.113.090076
This article has not been copyedited and formatted. The final version may differ from this version.
MOL #90076

Introduction

Synthetic pyrethroid insecticides were introduced into widespread use for the control of insects and disease vectors more than three decades ago. Pyrethroids account for approximately one-fourth of the worldwide insecticide market and the use of these compounds is increasing (Schleier and Peterson, 2011). Based on both their chemical structures and biological responses to acute exposure, pyrethroids are classified into two major groups: Type I and Type II. Type I pyrethroids lack a cyano group at the αcarbon of the 3-phenoxybenzyl alcohol moiety and produce hyperexcitation, tremors and convulsions (T syndrome), whereas Type II pyrethroids have a cyano group at the αcarbon and produce hypersensitivity, choreoathetosis, salivation, and seizures (CS syndrome). A few pyrethroids producing both tremors and salivation were classified as Type I/II (Soderlund, 2012; Casida and Durkin, 2013).

The primary molecular target underlying insecticidal activity and presumably mammalian neurotoxicity of pyrethroids are voltage-gated sodium channels (VGSC) (Soderlund, 2012; Casida and Durkin, 2013). Pyrethroids enhance sodium channel activity by shifting activation to more negative membrane potentials as well as by slowing channel inactivation. This action results in altered neuronal excitability characterized by *in vitro* and *in vivo* changes in neuronal firing rates (e.g. repetitive firing or depolarizing block of the neuron). In addition to their actions on VGSCs, pyrethroids also interact with other types of ion channels in a variety of *in vitro* systems, including altering the function of voltage-gated calcium (Ca^{2+}) channels and $GABA_A$ receptors (Clark and Symington, 2012; Soderlund, 2012; Casida and Durkin, 2013). It should be noted that all of these actions invariably require exposure to pyrethroid a concentrations $\geq$1 μM.

Molecular Pharmacology Fast Forward. Published on January 30, 2014 as DOI: 10.1124/mol.113.090076
This article has not been copyedited and formatted. The final version may differ from this version.
MOL #90076

Bifenthrin (**Fig. 1**) is one of the most potent commercialized pyrethroids to date, with LD_{50} values of about 53 mg/kg in female rats and 70 mg/kg in male rats following oral gavage (Wolansky et al., 2006; Wolansky and Harrill, 2008). Bifenthrin, as low as 10mg/kg, produces Type I pyrethroid-like episodes of head and whole body shakes, a strong and prolonged tremorigenic response, hyperthermia, vocalizations, prostration and, at doses > 28mg/kg, eventually triggers convulsions and death (Holton et al., 1997; Wolansky et al., 2007). This dose range corresponds to a brain concentration of bifenthrin of about 550-650 ng/g brain tissue (Scollon et al., 2011). The high dose effect is consistent with pyrethroid-induced perturbation of voltage-dependent Na^+ and Ca^{2+} fluxes at μM concentrations in primary cultured cortical neurons (Cao et al., 2011a; Cao et al., 2011b). However, at a threshold dose of 1.28 mg/kg, which corresponds to a brain concentration of roughly 30 ng/g brain tissue, bifenthrin decreases motor activity in rats (Wolansky et al., 2006; Scollon et al., 2011). These data suggest that bifenthrin can alter CNS physiology at doses much lower than those needed to induce tremors.

Extensive studies have been performed to elucidate the molecular mechanism and cellular effect of pyrethroids in cultured neurons. Previously we have demonstrated that at concentrations >1 μM, 9 out of 11 commercially used pyrethroids enhance Na^+ and Ca^{2+} fluxes with distinct potencies and efficacies (Cao et al., 2011a; Cao et al., 2011b) by a mechanism that is consistent with their reported actions on VGSC expressed in *Xenopus* oocytes (Choi and Soderlund, 2006) . For example, in mouse cortical neuronal cultures bifenthrin induces modest Na^+ and Ca^{2+} influx at concentrations above 3 μM, which can be eliminated by TTX pretreatment, demonstrating that bifenthrin is a low efficacy sodium channel agonist. Pyrethroids have also been demonstrated to act on Ca^{2+} or Cl^- channels

Molecular Pharmacology Fast Forward. Published on January 30, 2014 as DOI: 10.1124/mol.113.090076
This article has not been copyedited and formatted. The final version may differ from this version.
MOL #90076

(Clark and Symington, 2012; Soderlund, 2012), however, no direct evidence has been presented demonstrating that bifenthrin can interact with these channels. Furthermore, the possible effect of pyrethroids on neuronal network electrical activity has been investigated. Deltamethrin (0.1 μM) and permethrin (0.1 μM) both are able to increase electric spike activity in the absence of GABAergic inhibition (Meyer et al., 2008), however, bifenthrin appears without effect, even at a concentration of 50 μM (McConnell et al., 2012).

Murine primary cultured neurons mature to form synaptic networks and display spontaneous synchronized Ca^{2+} oscillations (Cao et al., 2012a). These spontaneous Ca^{2+} oscillations are dependent on the generation of action potentials and can be manifested by multiple Ca^{2+} signaling pathways (Dravid and Murray, 2004). Synchronous Ca^{2+} oscillations (SCO) are important in mediating neuronal development and activity dependent dendritic growth (Dolmetsch et al., 1998; Wayman et al., 2006). Genetic or environmental factors that interfere with activity dependent dendritic growth influence the functioning of neuronal networks (Pessah et al., 2010; Stamou et al., 2013).

In the present study, we identify a novel mechanism by which bifenthrin, at nanomolar concentrations, alters the patterns of SCO in primary mouse cortical neuronal cultures by amplifying glutamatergic glutamate receptor 5 (mGluR5) activity that alters CREB signaling and patterns of neurite outgrowth in the absence of detectable perturbation of VGSCs. To date, these are the most potent neurotoxic actions attributed to bifenthrin, and suggest that bifenthrin at low concentrations relevant to current exposures can persistently alter patterns of SCO and activity dependent neuronal cell growth and network development.

Molecular Pharmacology Fast Forward. Published on January 30, 2014 as DOI: 10.1124/mol.113.090076
This article has not been copyedited and formatted. The final version may differ from this version.
MOL #90076

Materials and Methods

Materials

Bifenthrin (purity: 99.1%, mix of isomers) was from Chemical Service, Inc. (West Chester, PA) (**Fig. 1**). Anti-p-CREB, anti-CREB and anti-MAP2 antibodies were from Cell Signaling Technology (Danvers, MA, USA). Odyssey Blocking Buffer and IRDye-labeled secondary antibody were from LI-COR Biotechnology (Lincoln, NE, USA). Fluo-4 and Alexa Fluor 488 conjugated goat anti-rabbit secondary antibody were from Life Technologies (Grand Island, NY, USA). TTX (tetrodotoxin), D-AP-5 (D-(-)-2-amino-5-phosphonopentanoic acid), MK-801 ((5*S*,10*R*)-(+)-5-methyl-10,11-dihydro-5*H*-dibenzo[*a*,*d*]cyclohepten-5,10-imine maleate), CNQX (6-cyano-7-nitroquinoxaline-2,3-dione), MPEP (2-methyl-6-(phenylethynyl)pyridine), nifedipine (3,5-dimethyl 2,6-dimethyl-4-(2-nitrophenyl)-1,4-dihydropyridine-3,5-dicarboxylate) were from Tocris Bioscience (Minneapolis, MN, USA).

Cortical neuronal cultures

The University of California Davis Animal Use and Care Committee approved this study, and animal experiments were conducted in accordance with the guidelines of Animal Use and Care of the National Institutes of Health. Cortical neurons were dissociated from the cortex from C57Bl/6J mouse pups at postnatal day 0–1 as described previously (Cao et al., 2011b). The dissociated neurons were maintained in Neurobasal complete medium (Neurobasal medium supplemented with NS21 (Chen, et al., 2010), 0.5 mM l-glutamine, and 4-(2-hydroxyethyl)-1-piperazineethanesulfonic acid [HEPES]) with 5% fetal bovine serum. The dissociated cortical cells were plated onto poly-l-lysine-coated (0.5 mg/ml, Sigma, St. Louis, MO, USA) clear-bottom, black wall, 96-well imaging plates (BD, Franklin Lakes, NJ) at densities of $1x10^5$/well for Ca^{2+} imaging and 2000/well for immunocytochemistry,

Molecular Pharmacology Fast Forward. Published on January 30, 2014 as DOI: 10.1124/mol.113.090076
This article has not been copyedited and formatted. The final version may differ from this version.
MOL #90076

respectively. For the western blot experiments, the dissociated cortical neurons were plated onto poly-l-lysine-coated 6-well plates at a density of $3x10^6$/well. The medium was changed twice a week by replacing half the volume of culture medium in the well with serum-free Neurobasal complete medium. The neurons were maintained at 37°C with 5% CO_2 and 95% humidity.

Measurement of synchronous intracellular Ca^{2+} oscillations

Cortical neurons at 9 days *in vitro* (DIV) were used to investigate how acute exposure to bifenthrin alters synchronous Ca^{2+} oscillations as described previously (Cao et al., 2012a). Briefly, the neurons were loaded with Fluo-4 for 1h at 37˚C in Locke's buffer (in mM; 8.6 HEPES, 5.6 KCl, 154 NaCl, 5.6 glucose, 1.0 $MgCl_2$, 2.3 CaCl2, and 0.0001 glycine, pH 7.4). After recording the baseline spontaneous Ca^{2+} oscillations for 3 min, vehicle or bifenthrin was added to the well using a programmable 96-channel pipetting robotic system, and the intracellular Ca^{2+} concentration ($[Ca^{2+}]_i$) was monitored for additional 50 min. The calculations for EC_{50} for changes in oscillatory frequency and peak transient amplitude were from data acquired between 30-40min after additions were made (ie, averages from a 10-min period). To test mechanisms influencing SCO activity, receptor-targeted inhibitors were added to designated wells after the Ca^{2+} response was induced by bifenthrin (0.1 μM).

To test the chronic influences, exposures of neurons to bifenthrin (0.01-1 μM) commenced 24 h after plating, and on 6 DIV the patterns of SCO measured as described above.

Membrane potential measurement

A membrane sensitive dye, FMPblue, was used to investigate whether bifenthrin can depolarize the membrane potential in 8-9 DIV neurons. Briefly, the neurons were loaded

Molecular Pharmacology Fast Forward. Published on January 30, 2014 as DOI: 10.1124/mol.113.090076
This article has not been copyedited and formatted. The final version may differ from this version.
MOL #90076

with 180 µl of FMPblue (1 vial diluted to 50 ml Lock's, Molecular Devices, Sunnyvale, CA, USA). After incubation with the dye for 30 min, the cells were excited at 510-545 nm and the fluorescent signals emitted at 565-625 nm were recorded. After recording basal fluorescence for 1 min, vehicle or bifenthrin (0.01-1.0 µM) was added to wells and the signals were recorded for an additional 40 min.

Measurement of neuronal Na^+, K^+ and Ca^{2+} channel currents

Cultured cortical neurons were voltage clamped by whole-cell patch-clamp using an EPC-10 amplifier and Pulse software (HEKA, Lambrecht/Pfalz, Germany). Cells were bathed in extracellular solution containing (in mM): 160 NaCl, 4.5 KCl, 1 $MgCl_2$, 2 $CaCl_2$ and 10 HEPES; pH was adjusted to 7.4 using NaOH (310 mOsm). Pipettes were pulled from 1.5 mm capillary tubing and filled with intracellular solution containing (in mM) either: 145 KF, 2 $MgCl_2$, 10 EGTA and 10 HEPES (pH adjusted to 7.2 with KOH; 300 mOsm) or 145 CsF, 3 KCl, 2 NaCl, 1 $MgCl_2$, 3 Na-ATP, 0.2 Na-GTP, 10 EGTA and 10 HEPES (pH adjusted to 7.4 with KOH; 303 mOsm). Pipette tip resistances were 2-4 MΩ. Series resistances of 3-10 MΩ were compensated 40-80%. All neurons were voltage clamped to a holding potential of -80 mV. Data analysis, fitting, and plotting were performed with IGOR-Pro (Wavemetrics, Lake Oswego, OR) and Origin 9.0 (OriginLab, Northampton, MA). Na^+ currents were elicited by 50-ms voltage steps from -80 to 0 mV applied every 10 s. Current decay and tail current were fitted with the following equation:

$$\mathrm{I} = \mathrm{A1} \times \exp(-\mathrm{t}/\tau 1) + \mathrm{A2} \times \exp(-\mathrm{t}/\tau 2) + \mathrm{C}$$

Where I is the current amplitude, t the time range of current chosen for fitting, τ_1, the fast time constant of inactivation, and τ_2 is the slow time constant of inactivation. A_1 and A_2 are

Molecular Pharmacology Fast Forward. Published on January 30, 2014 as DOI: 10.1124/mol.113.090076
This article has not been copyedited and formatted. The final version may differ from this version.
MOL #90076

the percentages of current inactivating with the fast and slow time constants, respectively, and C is the noninactivating current component.

K^+ currents were elicited by 200-ms voltage steps from -80 to 40 mV applied every 10 s. L929 cells stably expressing $mK_V3.1$ and $mK_V1.1$ were previously described (Grissmer et al., 1994). Experiments were performed with the same external and internal solutions as used for the cortical neurons.

Bifenthrin's influence on ryanodine receptor type 1 (RyR1) isolated from rabbit skeletal muscle was assessed in two ways, [^{3}H]ryanodine binding analysis and measurements of ionic current from single channels reconstituted in bilayer lipid membranes, as previously described (Pessah et al, 2010).

Immunocytochemistry and neurite outgrowth

Twenty-four hours after plating, cortical neurons were exposed to concentrations of bifenthrin ranging from 0.01 to 1.0 µM for 48h. After a brief wash with PBS, cells were fixed with 4% paraformaldehyde for 20 min and then permeabilized with 0.25% triton x-100 for 15 min. Following blocking with PBS with 10% BSA and 1% goat serum for 1h, cells were incubated with anti-MAP2 (1:1000) antibody in PBS containing 1% goat serum overnight at 4 ˚C. Cells were then incubated with Alexa Fluor 488-conjugated goat anti-rabbit secondary antibody (1:500) for 1 h at room temperature. After aspiration of the secondary antibody, 0.2mg/ml Hoechst 33342 was added to each well for 5 min to stain the nuclei. Pictures were recorded using an ImageXpress High Content Imaging System (Molecular Devices, Sunnyvale, CA) using a 10x objective with both FITC and DAPI filters. Nine adjacent sites (3x3) which cover ~60% of the center surface area were pictured for each well. Neurite outgrowth was then analyzed using MetaXpress Software (Molecular Devices, Sunnyvale,

Molecular Pharmacology Fast Forward. Published on January 30, 2014 as DOI: 10.1124/mol.113.090076
This article has not been copyedited and formatted. The final version may differ from this version.
MOL #90076

CA). The cell body was selected based on both DAPI and FITC staining by setting the maximal and minimal diameter and the minimal fluorescence intensity relative to the background from both channels. The neurite was traced automatically by setting the maximal width and minimal fluorescence intensity above background. The same criteria were applied to analyze the entire plate. The analyzed data were saved to the core computer facility and the neurons with neurites extending beyond the edge of the picture frame or neurite length shorter than 50 μm were excluded from analysis.

Western blot

The sample preparation for western blot was performed as described previously (Cao et al., 2012b). An equal amount of sample protein (20 μg) was loaded onto the wells of 10% SDS–PAGE gels and transferred to a nitrocellulose membrane by electroblotting. The membranes were blocked with Odyssey Blocking Buffer (LI-COR Biotechnology, Lincoln, NE, USA) in PBS buffer + 0.1% Tween-20 for 1.5–2 h at room temperature. After blocking, membranes were incubated overnight at 4˚C in anti-p-CREB (1:1000; Cell Signaling Technology, Danvers, MA, USA). The blots were washed and incubated with the IRDye (800CW)-labeled secondary antibody (1:10 000; LI-COR Biotechnology, Lincoln, NE, USA) for 1 h at room temperature. After washing with 0.1% Tween in PBS for five times, the membrane was scanned with the LI-COR Odyssey Infrared Imaging System (LI-COR Biotechnology, Lincoln, NE, USA). Densitometry was performed using the LI-COR Odyssey Infrared Imaging System application software 2.1. Membranes were stripped with NewBlot Nitro Stripping Buffer and reblotted for analysis of anti-CREB (1:1000; Cell Signaling Technology, Danvers, MA, USA).

Molecular Pharmacology Fast Forward. Published on January 30, 2014 as DOI: 10.1124/mol.113.090076
This article has not been copyedited and formatted. The final version may differ from this version.
MOL #90076

Data analysis

Graphing and statistical analysis were performed using GraphPad Prism software (Version 5.0, GraphPad Software Inc., San Diego, CA). EC_{50} value was determined by non-linear regression using a three parameter logistic equation. Statistical significance between different groups was calculated using Student's *t*-test or by an ANOVA and, where appropriate, a Dunnett's multiple comparison test; *p* values below 0.05 were considered statistically significant. EC_{50} value determination and statistics (ANOVA) for the electrophysiological experiments were performed with Origin 9.0 (OriginLab, Northampton, MA).

Molecular Pharmacology Fast Forward. Published on January 30, 2014 as DOI: 10.1124/mol.113.090076
This article has not been copyedited and formatted. The final version may differ from this version.
MOL #90076

Results

Acute exposure to nanomolar bifenthrin alters SCO patterns in cortical neurons

Bifenthrin was previously shown to induce modest Ca^{2+} influx at concentrations >3 μM (Cao et al., 2011a; Cao et al., 2011b). These studies focused on net Ca^{2+} influx associated with neuronal excitotoxicity, but not possible alternations of patterns of SCO that are important for activity dependent gene expression, neuronal cell growth and plasticity. We therefore performed directed studies to investigate whether bifenthrin at submicromolar concentrations influences Ca^{2+} dynamics and their possible mechanisms. Primary murine cortical neurons grown in 96-well plates were loaded with Fluo-4 at 8-9 DIV and cytoplasmic Ca^{2+} dynamics were monitored in real-time using FLIPR Tetra. Under these conditions, dissociated neuronal cultures form extensive networks that engage synchronized Ca^{2+} oscillations (**Fig. 2A, Top trace**) essential for promoting dendritic complexity and activity dependent plasticity (Chen et al., 2010; Cao et al., 2012a; Cao et al., 2012b). Addition of bifenthrin (0.01-1 μM) produced a concentration-dependent increase in the frequency of SCO having an EC_{50} value of 57.7 nM (31.9-104 nM, 95% confidential interval) that attained 270% of baseline at 1 μM (**Fig. 2A, Traces 2-8; Fig 2B**). Coincident with the increasing frequency of SCO, bifenthrin partially decreased the mean amplitude of the Ca^{2+} oscillations reaching 64% of control at 1 μM (**Fig. 2A&C**). The IC_{50} value for bifenthrin suppressing the mean amplitude of the Ca^{2+} oscillations was 83.4 nM (49.8-141.0 nM, 95% confidential interval) (**Fig. 2C**). To test whether the bifenthrin response on SCO was reversible, the cells were completely washed for 5 times with Lock's buffer after exposure to 0.1 μM bifenthrin for 30 min. Washing the cells itself has no detectable influence on the basal SCO (**Supplementary Fig. 1, upper black traces)**. However, the bifenthrin-augmented pattern

Molecular Pharmacology Fast Forward. Published on January 30, 2014 as DOI: 10.1124/mol.113.090076
This article has not been copyedited and formatted. The final version may differ from this version.
MOL #90076

of SCO was not fully reversible after washout, suggesting persistent alteration in the pattern of SCO after acute exposure to a low concentration of bifenthrin (**Supplementary Fig. 1, lower red traces**).

Nanomolar bifenthrin neither alters membrane potential nor voltage-gated currents

The FMPblue dye was used to examine whether bifenthrin alters the resting membrane potential of cortical neurons. After recording basal FMPblue fluorescence for 1 min, bifenthrin was added to the well and the signal was recorded for an additional 40 min. Bifenthrin at a concentration that caused a nearly 2-fold increase in SCO frequency (0.1 µM) had no detectable influence on membrane potential (**Fig. 3**). Even at concentrations as high as 1 µM, bifenthrin had negligible effect on the membrane potential (data not shown). As a positive control, application of KCl (10 mM) to the external bath showed that the FMPblue dye was capable of reporting even a modest (14 mV, calculated from Goldman–Hodgkin–Katz equation) shift in membrane depolarization (**Fig. 3**).

To more directly explore whether bifenthrin induced changes in Ca^{2+} oscillations might be due to direct effects on voltage-gated sodium channels, we tested the effect of bifenthrin on Na^{+} currents in cultured cortical neurons using whole-cell patch-clamp. As shown in **Figure 4A** bifenthrin concentrations of 10 and 100 µM drastically slowed inactivation during depolarization as evidenced by the broadening and incomplete inactivation of the Na^{+} current elicited by a 50 ms depolarizing step from -80 mV to 0 mV, while concentrations of 0.1 or 1 µM had no effect. Bifenthrin further delayed deactivation as shown by the large Na^{+} tail currents that became apparent following repolarization to -80 mV. This slow tail current, which constitutes an additional component to the normal fast tail current evoked upon repolarization, was very sensitive to bifenthrin and 0.1 µM already

Molecular Pharmacology Fast Forward. Published on January 30, 2014 as DOI: 10.1124/mol.113.090076
This article has not been copyedited and formatted. The final version may differ from this version.
MOL #90076

slightly changed the deactivation time constant τ_2 of its biexponential decay (**Fig. 4C**). However, since the physiological relevance of the tail current is not clear, we fitted separate EC_{50}s (**Fig. 4B**) for increasing the area under the current elicited by depolarization (16.8 ± 0.7 □M) and the area under the tail current (4.4 ± 0.4 μM) assuming the effect at 100 μM to be maximal. The more meaningful of these EC_{50}s representing the bifenthrin induced delay in VGSC inactivation is 275-fold higher than the EC_{50} for increasing SCO frequency. We further tested bifenthrin on cortical neuron K^+ currents as well as on heterologous expressed $K_v1.1$ and $K_v3.1$, two of the major delayed-rectifier type K^+ channels expressed in cortical neurons (Grissmer et al., 1994; Massengill et al., 1997; Goldberg et al., 2008), and found that 1 μM of bifenthrin had absolutely no effect on K_V currents (data not shown).

We tested if bifenthrin-triggered SCO patterns could be reversed by the addition of the L-type Ca^{2+} channel blocker nifedipine (10 μM). **Figures 5A&B** show that nifedipine neither affected basal SCO activity nor the activity modified by bifenthrin, discounting a possible contribution of L-type Ca^{2+} channel modulation in eliciting these effects of bifenthrin.

Finally, bifenthrin was also tested for possible influences towards ryanodine receptor activity as was recently reported for deltamethrin and selected Type II pyrethroids (Morisseau et al, 2009). Interestingly, bifenthrin ($\leq$ 1 μM) had no detectable influence on the gating activity of RyR1 channels reconstituted in bilayer lipid membranes nor altered the binding of [^{3}H]ryanodine to its high affinity sites (data not shown).

Metabotropic glutamate receptor 5 (mGluR 5) contributes to bifenthrin-modified SCO patterns

Molecular Pharmacology Fast Forward. Published on January 30, 2014 as DOI: 10.1124/mol.113.090076
This article has not been copyedited and formatted. The final version may differ from this version.
MOL #90076

Since SCO activity in cortical neurons was highly dependent on extracellular Ca^{2+} (data not shown), we investigated if Glu receptors contributed to bifenthrin-triggered alterations in SCO. Although MPEP (1 μM), a selective antagonist of mGluR 5, had no significant effect on basal SCO patterns, it produced a significant 60±8% amelioration of bifenthrin-triggered SCO patterns (**Fig. 5C)**. MPEP had no effect on the bifenthrin-induced decrease in the amplitude of SCO (**Fig. 5D**). Both AP-5 (50 μM) and MK801 (1 μM), competitive and noncompetitive antagonists of NMDAR, respectively, partially reversed bifenthrin-triggered SCO frequency (**Fig. 5E&G**). AP-5 reduced basal SCO frequency by 69±12% and bifenthrin-triggered SCO frequency by 78±5% (**Fig. 5E**). Similarly, MK801, reduced basal SCO by 49±14% and bifenthrin-triggered SCO frequency by 47±14% (**Fig. 5G**). MK801 and AP-5 alone also dramatically inhibited the amplitude of basal SCO by 69±4% and 71±4% of basal, respectively (**Fig. 5F&H**). Both MK801 and AP5 further inhibited bifenthrin-induced decrease in the amplitude of SCOs (**Fig. 5F&H**).

Sub-acute exposure to bifenthrin persistently alters SCO patterns

We next examined if more prolonged exposure to bifenthrin also persistently altered the SCO patterns. Cortical neurons were exposed to the vehicle or various concentrations of bifenthrin (0.01-0.30 μM) for 6 days commencing 24 h after plating. After washout of bifenthrin, cells were loaded with Fluo-4 for 1h. Following five washes the cell plate was transferred to the FLIPR Tetra imager and SCO were recorded. Chronic exposure to bifenthrin produced a persistent increase in SCO frequency (**Fig. 6 A and B**) and reduction in SCO amplitude (**Fig. 6A &C**) compared to vehicle control despite the extensive washout protocol (**Fig. 6**). Bifenthrin increased the frequency of SCO with an EC_{50} value of 52.8 nM (25.1-110.1 nM, 95% CI) and was associated with diminished oscillation amplitude having

Molecular Pharmacology Fast Forward. Published on January 30, 2014 as DOI: 10.1124/mol.113.090076
This article has not been copyedited and formatted. The final version may differ from this version.
MOL #90076

an IC_{50} value of 42.7 nM (25.3-72 nM, 95%CI) (**Fig. 6B&C**).

Nanomolar bifenthrin stimulates CREB phosphorylation

Ca^{2+} influx mediated by mGluR 5 glutamatergic neurotransmission is known to promote CREB phosphorylation that in turn stimulates a number of genes involved in normal activity-dependent plasticity (Bengtson and Bading, 2012), as well as environmentally triggered alterations of dendritic architecture (Jabba et al., 2010; Wayman et al., 2012). We therefore examined whether bifenthrin-induced changes in the pattern of SCO were sufficient to increase CREB phosphorylation on Ser 133. Western blot analysis demonstrated that exposure to bifenthrin (0.1 μM) enhanced p-CREB in a time dependent manner (**Fig. 7A&B**). Given MPEP partially ameliorated bifenthrin enhanced SCO activity, we tested if MPEP could also diminish bifenthrin stimulated CREB phosphorylation. After pre-incubation with MPEP (1μM) or vehicle (0.01%DMSO) for 15min, the neurons were then treated with bifenthrin (0.1μM) or vehicle (0.01%DMSO) for 3h. Western blot analysis showed that MPEP significantly inhibited bifenthrin-stimulated CREB phosphorylation without altering basal CREB phosphorylation (**Fig. 7C&D**).

Nanomolar bifenthrin alters neurite growth

Given the increased level of the p-CREB soon after exposure of cortical neurons to bifenthrin, we examined whether nanomolar bifenthrin was sufficient to influence neuronal cell growth. **Figure 8** showed that 48 h after commencing exposure, bifenthrin promoted neurite growth at 3 DIV in a concentration dependent manner between 0.01 and 0.1 μM (**Fig. 8**). Interestingly concentrations >0.1 μM, the concentration that elicited the greatest neurite growth, produced a trend for smaller neurites, although not statistically different from the 0.1 μM bifenthrin exposure (**Fig. 8B**). We hypothesized that bifenthrin stimulated neurite

Molecular Pharmacology Fast Forward. Published on January 30, 2014 as DOI: 10.1124/mol.113.090076
This article has not been copyedited and formatted. The final version may differ from this version.

outgrowth was a consequence of its ability to amplify mGluR 5 dependent SCO activity. Although MPEP (1μM) had no significant influence on the basal neurite outgrowth, this mGluR 5 antagonist completely normalized bifenthrin-triggered response (**Fig. 8C&D**).

Molecular Pharmacology Fast Forward. Published on January 30, 2014 as DOI: 10.1124/mol.113.090076
This article has not been copyedited and formatted. The final version may differ from this version.
MOL #90076

Discussion

In this study, we demonstrate that bifenthrin, at concentrations well below those that influence neuronal membrane potential and delay Na^+ channel inactivation (<1 μM), is capable of altering SCO that are essential for normal activity dependent growth of cortical neurons. It is well known that bifenthrin and related pyrethroid insecticides influence axonal voltage-gated Na^+ channels by delaying their inactivation and producing a significant tail current, and as such this mechanism is currently accepted as the primary mechanism for both insecticidal activity and mammalian neurotoxicity (Clark and Symington, 2012; Soderlund, 2012; Casida and Durkin, 2013). Currently the U.S. EPA proposes that all pyrethroids share a common mechanism for promoting impaired motor activity and therefore present a cumulative human health risk (U.S. EPA, 2011). However, neurotoxicological symptoms in mammalian models vary greatly among individual pyrethroids and differences in their toxicokinetics are insufficient to predict divergent behavioral responses (Wolansky *et al*., 2006; Starr et al., 2012). The current results indicate that, at least for bifenthrin, alterations in the patterns of SCO are independent of voltage-gated Na^+ channel modulation and occur at concentrations approximately two log units below those required for altering neuronal membrane potential. In support of an alternative mechanism, bifenthrin does not alter the spontaneous electric activity of cortical neurons measured in multiple electrode arrays (MEA; data not shown), a finding consistent with an independent report using cortical neuronal cultures (McConnell et al., 2012). Thus the newfound mechanism for bifenthrin may have implications for understanding differences in the potency and pattern of pyrethroid neurotoxicity. For example, bifenthrin differs little from permethrin in structure and physicochemical properties, yet bifenthrin has a 10- to 100-fold greater oral toxicity, which

Molecular Pharmacology Fast Forward. Published on January 30, 2014 as DOI: 10.1124/mol.113.090076
This article has not been copyedited and formatted. The final version may differ from this version.
MOL #90076

cannot be accounted for by differential activity at voltage-gated Na^+ channels (Wolansky and Harrill, 2008).

Since bifenthrin-altered SCO patterns are sufficient to modify CREB phosphorylation and the early growth trajectory of developing cortical neurons in culture, these results raise questions as to whether certain pyrethroids, such as bifenthrin, engage other primary molecular targets at concentrations much lower than those needed to modify voltage-gated Na^+ channels. Mechanisms that alter the integrity of SCO may not only contribute to higher acute toxicity, but may also affect more chronic neurodevelopmental outcomes related to long-term changes in Ca^{2+}-dependent processes including activity dependent dendritic growth regulated by CREB-dependent signaling pathways (Wayman et al, 2006). The observation that bifenthrin persistently alters SCO patterns after prolonged (6 day) exposure indicates that this pyrethroid could alter Ca^{2+} regulated pathways over the critical neurodevelopmental timeframe.

Although we failed to delineate the direct molecular targets for bifenthrin that elicit altered patterns of SCO, our data suggest that bifenthrin augments mGluR 5 signaling since an mGluR 5 receptor antagonist, MPEP, produced a maximal suppression in the bifenthrin-augmented SCO frequency without affecting the basal spontaneous Ca^{2+} oscillations frequency. This is consistent with previous reports that have demonstrated metabotropic glutamate (Glu) receptors signaling pathways regulate SCO behavior (Dravid and Murray, 2004; Koga et al., 2010). We also show that both competitive and non-competitive NMDA receptors antagonists, AP5 and MK801, suppress both basal and bifenthrin-augmented SCO activity. However, increased mGluR 5 activity cannot fully explain how bifenthrin alters

Molecular Pharmacology Fast Forward. Published on January 30, 2014 as DOI: 10.1124/mol.113.090076
This article has not been copyedited and formatted. The final version may differ from this version.
MOL #90076

SCO activity since metabotropic glutamate receptor antagonists could not recover the SCO baseline amplitude.

Bifenthrin-augmented Ca^{2+} signaling is sufficient to rapidly increase the phosphorylation of CREB and neurite extension. Consistent with the inhibition of SCO activity of MPEP, bifenthrin response on CREB phosphorylation and neurite outgrowth is also dependent on the amplification of the mGluR 5 activity since both outcomes are mitigated by MPEP. Activity-dependent calcium signaling has been shown to regulate dendritic growth and branching (Konur and Ghosh, 2005), which is dependent on the phosphorylation of CREB (Wayman et al., 2012). Small to moderate amplification of Ca^{2+} signaling stimulates dendritic growth while excessive Ca^{2+} influx may stall dendritic growth (Gomez and Spitzer, 2000; Hui et al., 2007). The concentration-dependent profile of bifenthrin-triggered neurite outgrowth therefore is consistent with previously reported mechanisms responsible for regulating activity-dependent dendritic growth (Gomez and Spitzer, 2000; Hui et al., 2007).

A number of pyrethroids have also been demonstrated to interact with $GABA_A$ receptors and Ca^{2+} channels (Clark and Symington, 2012; Soderlund, 2012). However, the bifenthrin's effect on SCO was unlikely from an interaction with $GABA_A$ receptors. Bicuculline, a competitive $GABA_A$ antagonist, was reported to increase the spike rate using MEA recording in cortical neurons (McConnell et al., 2012). In addition, we found that both bicuculline and picrotoxin increased the synchronicity of neuronal firing in cortical neuronal cultures (data not shown). However, bifenthrin fails to alter the spike rate and firing synchronicity. Bifenthrin-triggered alterations in SCO are also unlikely induced by direct interaction with Ca^{2+} channels since nifedipine has no effect on bifenthrin-augmented SCO,

Molecular Pharmacology Fast Forward. Published on January 30, 2014 as DOI: 10.1124/mol.113.090076
This article has not been copyedited and formatted. The final version may differ from this version.
MOL #90076

and we found no detectable influences of ryanodine receptor RyR1, as previously reported for deltamethrin (Morisseau et al 2009). Collectively, the current data are consistent with a previous report in which no direct interaction of bifenthrin with $GABA_A$ receptor or Ca^{2+} channels was observed (Burr and Ray, 2004).

In the 1999 National Health and Nutrition Examination Survey (NHANES), over 70% of a nationally representative sample of persons six years or older had detectable levels of pyrethroid metabolites in their urine (Barr et al., 2010). Although pyrethroids are generally thought to be rapidly metabolized, and therefore are unlikely to bioaccumulate in breast milk, several recent studies have found that pyrethroid levels vary greatly in human breast milk, ranging from <1 to 2000 ng g^{-1} depending on geographic location and insecticide use patterns (Sereda et al., 2009; Weldon et al., 2011; Corcellas et al., 2012). For example, a recent analysis of pyrethroids in human breast milk indicated that bifenthrin is most abundant in Brazilian samples, whereas λ-cyhalothrin and permethrin are most abundant in Colombian and Spanish samples, respectively (Corcellas et al., 2012). In this study the mean bifenthrin levels ranged from 1.44 to 2.8 ng g^{-1} (lipid weight) and maximum levels approached 7.48 ng g^{-1}. The bifenthrin concentration even in these highly exposed individuals would be below the minimum effective concentration (10 nM) that alters neurite outgrowth (**Fig. 8)**. However, considering the very low solubility of bifenthrin in aqueous media (log P 6.4) (Schleier and Peterson, 2011), the actual concentration of bifenthrin in the culture medium at the time measurements of neurite length and SCO properties after "chronic" exposures would be expected to be lower than nominal concentrations at the start of exposures.

Molecular Pharmacology Fast Forward. Published on January 30, 2014 as DOI: 10.1124/mol.113.090076
This article has not been copyedited and formatted. The final version may differ from this version.
MOL #90076

The present results also raise the important question whether exposure to bifenthrin could produce additive effects with other pyrethroids (Starr et al., 2012). It is also possible that the effects of bifenthrin may be additive with exposure to persistent chemicals such as non-dioxin like polychlorinated biphenyls (NDL PCBs) (Pessah et al., 2010) and/or genetic mutations known to produce abnormal SCO activity, dendritic and synaptic architecture and network connectivity (Stamou et al., 2013). For example, Fragile X mental retardation, a neurodevelopment disorder caused by loss of fragile X mental retardation protein (FMRP), is the most widespread single-gene cause of developmental disorders, including autism (Hagerman and Hagerman, 2013). In fragile X mental retardation 1 gene KO mouse model, enhanced mGluR 5 signaling has been demonstrated and contributes to long-term synaptic depression during synaptic transmission. Such disturbances in mGluR 5 signaling are thought to elicit cognitive as well as syndromic features of fragile X syndrome (Huber et al., 2002; Bear et al., 2004; Dolen and Bear, 2008), and *FMR1* premutation (Chen et al., 2010; Cao et al., 2012b; Liu et al., 2012). Our *in vitro* observation that nanomolar bifenthrin alters neuronal Ca^{2+} dynamics and mGluR 5 signaling activity with consequential changes in neurite outgrowth, provides evidence for a new paradigm in understanding how certain pyrethroids might influence health outcomes that involve abnormal neuronal network development associated with developmental disorders.

Molecular Pharmacology Fast Forward. Published on January 30, 2014 as DOI: 10.1124/mol.113.090076
This article has not been copyedited and formatted. The final version may differ from this version.
MOL #90076

Author Contributions:

Participated in research design: Cao, Wulff, Pessah

Conducted experiments: Cao, Cui, Nguyen, Jenkins,

Performed data analysis: Cao, Cui, Nguyen, Jenkins, Wulff, Pessah

Wrote or contributed to writing the manuscript: Cao, Cui, Nguyen, Wulff, Pessah

Molecular Pharmacology Fast Forward. Published on January 30, 2014 as DOI: 10.1124/mol.113.090076
This article has not been copyedited and formatted. The final version may differ from this version.
MOL #90076

References

Barr DB, Olsson AO, Wong LY, Udunka S, Baker SE, Whitehead RD, Magsumbol MS, Williams BL and Needham LL (2010) Urinary concentrations of metabolites of pyrethroid insecticides in the general U.S. population: National Health and Nutrition Examination Survey 1999-2002. *Env Health Perspect* **118:**742-748.

Bear MF, Huber KM and Warren ST (2004) The mGluR theory of fragile X mental retardation. *Trends Neurosci* **27:**370-377.

Bengtson CP, Bading H. (2012) Nuclear calcium signaling. *Adv Exp Med Biol* 970:377-405.

Burr SA and Ray DE (2004) Structure-activity and interaction effects of 14 different pyrethroids on voltage-gated chloride ion channels. *Toxicological sciences : an official journal of the Society of Toxicology* **77:**341-346.

Cao Z, Hammock BD, McCoy M, Rogawski MA, Lein PJ and Pessah IN (2012a) Tetramethylenedisulfotetramine alters Ca(2)(+) dynamics in cultured hippocampal neurons: mitigation by NMDA receptor blockade and GABA(A) receptor-positive modulation. *Tox Sci* **130:**362-372.

Cao Z, Hulsizer S, Tassone F, Tang HT, Hagerman RJ, Rogawski MA, Hagerman PJ and Pessah IN (2012b) Clustered burst firing in FMR1 premutation hippocampal neurons: amelioration with allopregnanolone. *Human Mol Gen* **21:**2923-2935.

Cao Z, Shafer TJ, Crofton KM, Gennings C and Murray TF (2011a) Additivity of pyrethroid actions on sodium influx in cerebrocortical neurons in primary culture. *Env Health Perspect* **119:**1239-1246.

Cao Z, Shafer TJ and Murray TF (2011b) Mechanisms of pyrethroid insecticide-induced stimulation of calcium influx in neocortical neurons. *J Pharm Exper Ther* **336:**197-

205.

Casida JE, Durkin KA (2013) Neuroactive insecticides: targets, selectivity, resistance, and secondary effects. *Annu Rev Entomol* **58:**99-117.

Chen Y, Tassone F, Berman RF, Hagerman PJ, Hagerman RJ, Willemsen R and Pessah IN (2010) Murine hippocampal neurons expressing Fmr1 gene premutations show early developmental deficits and late degeneration. *Human Mol Gen* **19:**196-208.

Choi JS and Soderlund DM (2006) Structure-activity relationships for the action of 11 pyrethroid insecticides on rat Nav 1.8 sodium channels expressed in Xenopus oocytes. *Tox Appl Pharm* **211:**233-244.

Clark JM and Symington SB (2012) Advances in the mode of action of pyrethroids. *Top Curr Chem* **314:**49-72.

Corcellas C, Feo ML, Torres JP, Malm O, Ocampo-Duque W, Eljarrat E, Barceló D (2012) Pyrethroids in human breast milk: occurrence and nursing daily intake estimation. *Environ Int* **47:**17-22.

Dolen G and Bear MF (2008) Role for metabotropic glutamate receptor 5 (mGluR5) in the pathogenesis of fragile X syndrome. *J Physiol* **586:**1503-1508.

Dolmetsch RE, Xu K and Lewis RS (1998) Calcium oscillations increase the efficiency and specificity of gene expression. *Nature* **392:**933-936.

Dravid SM and Murray TF (2004) Spontaneous synchronized calcium oscillations in neocortical neurons in the presence of physiological [Mg(2+)]: involvement of AMPA/kainate and metabotropic glutamate receptors. *Brain Res* **1006:**8-17.

Goldberg EM, Clark BD, Zagha E, Nahmani M, Erisir A and Rudy B (2008) K+ channels at the axon initial segment dampen near-threshold excitability of neocortical fast-spiking

GABAergic interneurons. *Neuron* **58:**387-400.

Gomez TM and Spitzer NC (2000) Regulation of growth cone behavior by calcium: new dynamics to earlier perspectives. *J Neurobiol* **44:**174-183.

Grissmer S, Nguyen AN, Aiyar J, Hanson DC, Mather RJ, Gutman GA, Karmilowicz MJ, Auperin DD and Chandy KG (1994) Pharmacological characterization of five cloned voltage-gated K+ channels, types Kv1.1, 1.2, 1.3, 1.5, and 3.1, stably expressed in mammalian cell lines. *Mol Pharmacol* **45:**1227-1234.

Hagerman PJ and Hagerman RJ (2013) Advances in clinical and molecular understanding of the FMR1 premutation and fragile X-associated tremor/ataxia syndrome. *Lancet Neurol* **12:**786-98.

Holton JL, Nolan CC, Burr SA, Ray DE and Cavanagh JB (1997) Increasing or decreasing nervous activity modulates the severity of the glio-vascular lesions of 1,3-dinitrobenzene in the rat: effects of the tremorgenic pyrethroid, Bifenthrin, and of anaesthesia. *Acta Neuropath* **93:**159-165.

Huber KM, Gallagher SM, Warren ST and Bear MF (2002) Altered synaptic plasticity in a mouse model of fragile X mental retardation. *Proc Nat Acad Sci USA* **99:**7746-7750.

Hui K, Fei GH, Saab BJ, Su J, Roder JC and Feng ZP (2007) Neuronal calcium sensor-1 modulation of optimal calcium level for neurite outgrowth. *Dev* **134:**4479-4489.

Jabba SV, Prakash A, Dravid SM, Gerwick WH and Murray TF (2010) Antillatoxin, a novel lipopeptide, enhances neurite outgrowth in immature cerebrocortical neurons through activation of voltage-gated sodium channels. *J Pharm Exper Therap* **332:**698-709.

Koga K, Iwahori Y, Ozaki S and Ohta H (2010) Regulation of Spontaneous Ca2+ Spikes by Metabotropic Glutamate Receptors in Primary Cultures of Rat Cortical Neurons. *J*

Neurosci Res **88:**2252-2262.

Konur S and Ghosh A (2005) Calcium signaling and the control of dendritic development. *Neuron* **46:**401-405.

Liu J, Koscielska KA, Cao Z, Hulsizer S, Grace N, Mitchell G, Nacey C, Githinji J, McGee J, Garcia-Arocena D, Hagerman RJ, Nolta J, Pessah IN and Hagerman PJ (2012) Signaling defects in iPSC-derived fragile X premutation neurons. *Human Mol Gen* **21:**3795-3805.

Massengill JL, Smith MA, Son DI and O'Dowd DK (1997) Differential expression of K4-AP currents and Kv3.1 potassium channel transcripts in cortical neurons that develop distinct firing phenotypes. *J Neurosci* **17:**3136-3147.

McConnell ER, McClain MA, Ross J, Lefew WR and Shafer TJ (2012) Evaluation of multi-well microelectrode arrays for neurotoxicity screening using a chemical training set. *Neurotoxicol* **33:**1048-1057.

Meyer DA, Carter JM, Johnstone AF and Shafer TJ (2008) Pyrethroid modulation of spontaneous neuronal excitability and neurotransmission in hippocampal neurons in culture. *Neurotoxicol* **29:**213-225.

Pessah IN, Cherednichenko G, Lein PJ (2010) Minding the calcium store: Ryanodine receptor activation as a convergent mechanism of PCB toxicity. *Pharmacol Ther* **125:**260-85.

Roberts EM, English PB, Grether JK, Windham GC, Somberg L and Wolff C (2007) Maternal residence near agricultural pesticide applications and autism spectrum disorders among children in the California Central Valley. *Env Health Perspec* **115:**1482-1489.

Schleier JJ and Peterson RKD (2011) Pyrethrins and Pyrethroid Insecticides, in RSC Green Chemistry No. 11 Green Trends in Insect Control (Oscar López O and Fernández-Bolaños JG, Eds) pp 94-131.

Scollon EJ, Starr JM, Crofton KM, Wolansky MJ, DeVito MJ and Hughes MF (2011) Correlation of tissue concentrations of the pyrethroid bifenthrin with neurotoxicity in the rat. *Toxicology* **290:**1-6.

Sereda B, Bouwman H, Kylin H (2009) Comparing water, bovine milk, and indoor residual spraying as possible sources of DDT and pyrethroid residues in breast milk. *J Toxicol Environ Health A* **72:**842–51.

Soderlund DM (2012) Molecular mechanisms of pyrethroid insecticide neurotoxicity: recent advances. *Arch Toxicol* **86:**165-181.

Stamou M, Streifel KM, Goines PE, Lein PJ (2013) Neuronal connectivity as a convergent target of gene × environment interactions that confer risk for Autism Spectrum Disorders. *Neurotoxicol Teratol* **36:**3-16.

Starr JM, Scollon EJ, Hughes MF, Ross DG, Graham SE, Crofton KM, Wolansky MJ, Devito MJ, Tornero-Velez R (2012) Environmentally relevant mixtures in cumulative assessments: an acute study of toxicokinetics and effects on motor activity in rats exposed to a mixture of pyrethroids. *Toxicol Sci* **130:**309-18.

Tanaka T, Saito H and Matsuki N (1996) Intracellular calcium oscillation in cultured rat hippocampal neurons: a model for glutamatergic neurotransmission. *Jap J Pharmacol* **70:**89-93.

U.S. EPA. (2011). Pyrethrins/Pyrethroids Cumulative Risk Assessment; Notice of Availability. EPA-HQ-OPP-2011-0746; FRL-8888–9. U.S. Environmental Protection

Agency, Research Triangle Park, NC.

Wayman GA, Bose DD, Yang DR, Lesiak A, Bruun D, Impey S, Ledoux V, Pessah IN and Lein PJ (2012) PCB-95 Modulates the Calcium-Dependent Signaling Pathway Responsible for Activity-Dependent Dendritic Growth. *Env Health Perspec* **120:**1003-1009.

Wayman GA, Impey S, Marks D, Saneyoshi T, Grant WF, Derkach V and Soderling TR (2006) Activity-dependent dendritic arborization mediated by CaM-kinase I activation and enhanced CREB-dependent transcription of Wnt-2. *Neuron* **50:**897-909.

Weldon RH, Barr DB, Trujillo C, Bradman A, Holland N, Eskenazi B (2011) A pilot study of pesticides and PCBs in the breast milk of women residing in urban and agricultural communities of California. *J Environ Monit* **13:**3136-44.

Wolansky MJ, Gennings C and Crofton KM (2006) Relative potencies for acute effects of pyrethroids on motor function in rats. *Tox Sci* **89:**271-277.

Wolansky MJ and Harrill JA (2008) Neurobehavioral toxicology of pyrethroid insecticides in adult animals: a critical review. *Neurotox Teratol* **30:**55-78.

Wolansky MJ, McDaniel KL, Moser VC and Crofton KM (2007) Influence of dosing volume on the neurotoxicity of bifenthrin. *Neurotox Teratol* **29:**377-384.

Molecular Pharmacology Fast Forward. Published on January 30, 2014 as DOI: 10.1124/mol.113.090076
This article has not been copyedited and formatted. The final version may differ from this version.

Footnotes

This work was supported by the National Institute of Environmetal Health Sciences [1P01 ES011269, 1R01 ES020392], the National Institute of Neurological Disorders and Stroke [1U54 NS079202], and the U.S. Environmental Protection Agency EPA [8354320].

Zhengyu Cao current address: State Key Laboratory of Natural Medicines, Department of Complex Prescription of TCM, China Pharmaceutical University, Nanjing, P.R. China, 211198

Molecular Pharmacology Fast Forward. Published on January 30, 2014 as DOI: 10.1124/mol.113.090076
This article has not been copyedited and formatted. The final version may differ from this version.

Legends of Figures

Figure 1 | Chemical structure of bifenthrin.

Figure 2 | Bifenthrin-induced Ca^{2+} dysregulation in cortical neurons. (A) Representative traces showing how acute exposure to bifenthrin (0.01-1 μM) influences Ca^{2+} fluctuations in cortical neurons at 8-9 DIV as a function of time. Bifenthrin produces a robust increase in the frequency of Ca^{2+} oscillations accompanied by the slightly decreased Ca^{2+} oscillations amplitude. (B), Concentration-response relationships for bifenthrin-stimulated increase in the frequency of Ca^{2+} oscillation. The EC_{50} value for bifenthrin-stimulated increase in the frequency of Ca^{2+} oscillation frequency is 57.7nM. (C), Concentration-response relationships for bifenthrin-stimulated decrease in the amplitude of Ca^{2+} oscillation. The EC_{50} value for bifenthrin-stimulated decrease in the amplitude of Ca^{2+} oscillation frequency is 83.4nM. These data were averaged from a time period between 30-40 min after addition of bifenthrin. Each data point represents Mean±SEM (n>20 well) from five independent cultures.

Figure 3| Bifenthrin has no effect on membrane potential in cortical neurons. Influence of bifenthrin (0.1 μM) or KCl (10mM, positive control) on the rest membrane potential as a function of time. KCl produces a significant depolarization of the cortical neurons reflected by increased FMPblue fluorescence signals. However, bifenthrin has no response on the resting membrane potential. This experiment was repeated twice each with five replicates with similar results.

Molecular Pharmacology Fast Forward. Published on January 30, 2014 as DOI: 10.1124/mol.113.090076
This article has not been copyedited and formatted. The final version may differ from this version.
MOL #90076

Figure 4 | Low bifenthrin concentrations do not affect cortical neuron Na^+ currents, while high concentrations delay inactivation. (A) Representative Na^+ current recording showing the effect of vehicle control (DMSO) followed by increasing concentrations of bifenthrin (0.1, 1, 10, and 100 µM). Na^+ currents were elicited by 50 ms voltage steps from -80 to 0 mV followed by a 50 ms step back to -80 mV. Under these recording conditions higher bifenthrin concentrations delayed inactivation and induced a slow tail current visible following repolarization to -80 mV. (B) Concentration-response curves for increasing the charge during depolarization (= delay of Nav channel inactivation) or following repolarization (= increase of tail current). Data were normalized to the maximal response elicited with the highest bifenthrin concentration. (C) Inactivation time constants for decay of the current and the tail current. Experiments were repeated on three independent cells with similar results and data are presented as Mean±SD. Statistical significance between different groups was calculated using Student's t-test.

Figure 5 | mGluR5-NMDAR mediated neurotransmission, but not L-Type Ca^{2+} channels contributes to bifenthrin-triggered SCO patterns. After exposure to vehicle or bifenthrin for 30 min, cortical neurons were exposed to either an L-type Ca^{2+} channel blocker, nifedipine (1 µM) (A, B), the specific mGluR 5 antagonist MPEP (1 µM) (C, D), MK801 (1 µM), a noncompetitive antagonist of MNDAR (E, F) or the competitive MNDAR antagonist AP-5 (50 µM) (G,H) to assess further modification/reversal of SCO activity. The data shown were averaged from a 10 min period immediately after addition of vehicle or candidate inhibitors. Data represent Mean±SEM (n> 12) from at least two independent cultures performed in at least triplicates. Statistical significance between different groups was

Molecular Pharmacology Fast Forward. Published on January 30, 2014 as DOI: 10.1124/mol.113.090076
This article has not been copyedited and formatted. The final version may differ from this version.

calculated using an ANOVA followed by a Dunnett's multiple comparison test (**, $p<0.01$, bifenthrin *vs.* vehicle; ##, $p<0.01$, inhibitor vs. vehicle; $$, $p<0.01$, inhibitor + bifenthrin *vs.* bifenthrin).

Figure 6 | Chronic exposure to bifenthrin persistently alters SCO in cortical neurons. (A) Representative traces showing that chronic exposure (7 days) to bifenthrin (0.01-0.3 µM) influences SCO patterns in cortical neurons at 8 DIV. Bifenthrin produces a robust increase in the frequency of SCO and is accompanied by a modest decrease in amplitude; (B) Concentration-response relationships for bifenthrin-stimulated increase in the frequency of SCO, with an EC_{50} value of 52.7nM. (C) Concentration-response relationships for bifenthrin-triggered decrease in SCO amplitude, with an EC_{50} of 42.7nM. These data were averaged from a recording time period between 0-10min. This experiment was repeated three times each from recordings from five culture wells with similar results.

Figure 7 | Bifenthrin enhaced p-CREB is dependent on the mGluR 5 activity. (A) Representative western blot for bifenthrin (0.1 µM)-stimulated CREB phosphorylation (p-CREB) in 8-9 DIV cortical neurons as a function of time post-treatment. (B) Quantification of bifenthrin-induced CREB phosphorylation. Each data point represents Mean±SEM (n=4) from two independent cultures, each time performed in duplicate. (C) Representative western blot for MPEP (1µM) on bifenthrin (0.1 µM)-stimulated CREB phosphorylation (p-CREB) in 8-9 DIV cortical neurons. (D) Quantification of MPEP response of MPEP on bifenthrin-induced CREB phosphorylation. Each data point represents Mean±SEM (n=3) from two independent cultures. Statistical significance between different groups

Molecular Pharmacology Fast Forward. Published on January 30, 2014 as DOI: 10.1124/mol.113.090076
This article has not been copyedited and formatted. The final version may differ from this version.
MOL #90076

was calculated using an ANOVA and followed by a Dunnett's multiple comparison test (*, $p<0.05$; **, $p<0.01$, bifenthrin *vs.* vehicle; $^{\#\#}$, $p<0.01$, bifenthrin vs. MPEP+bifenthrin).

Figure 8 | Bifenthrin altered the neurite outgrowth is dependent on the mGluR 5 activity in cortical neurons. (A) Representative neurons stained with MAP2 and Hoechst 33342 after exposure to vehicle (0.01%DMSO) or increasing concentrations of bifenthrin (0.01-1.0 µM) for 48h (neurons were fixed and stained on 3 DIV). (B) Quantification of the total neurite length/cell after vehicle and bifenthrin exposure. Bifenthrin produces a biphasic response in the neurite outgrowth, which peaked at 0.1 µM. (C) Representative neurons stained with MAP2 and Hoechst 33342 after exposure to vehicle (0.02%DMSO), MPEP (1µM), bifenthrin (0. 1µM) or MPEP+bifenthrin for 48h. MPEP was added to the culture medium 15 min before bifenthrin addition. (D) Quantification of the total neurite length/cell after MPEP, bifenthrin or MPEP+bifenthrin exposure. The experiments were repeated on two separate culture days with similar results. Statistical significance between different groups was calculated using an ANOVA and followed by a Dunnett's multiple comparison test (*, $p<0.05$, **, $p<0.01$, bifenthrin *vs*. vehicle, $^{\#\#}$, bifenthrin+MEPE *vs.* bifenthrin).

Molecular Pharmacology Fast Forward. Published on January 30, 2014 as DOI: 10.1124/mol.113.090076
This article has not been copyedited and formatted. The final version may differ from this version.

Figures

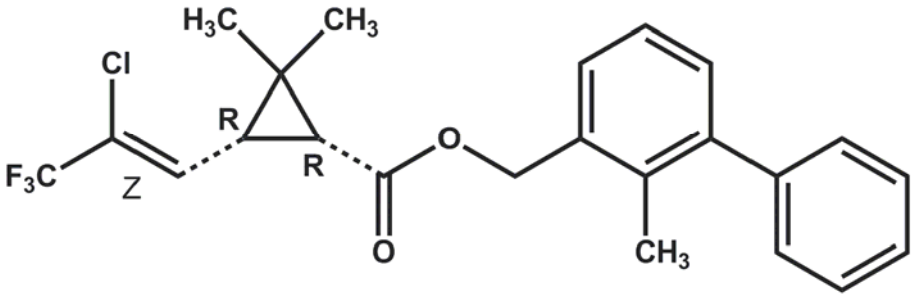

Figure 1

Molecular Pharmacology Fast Forward. Published on January 30, 2014 as DOI: 10.1124/mol.113.090076
This article has not been copyedited and formatted. The final version may differ from this version.

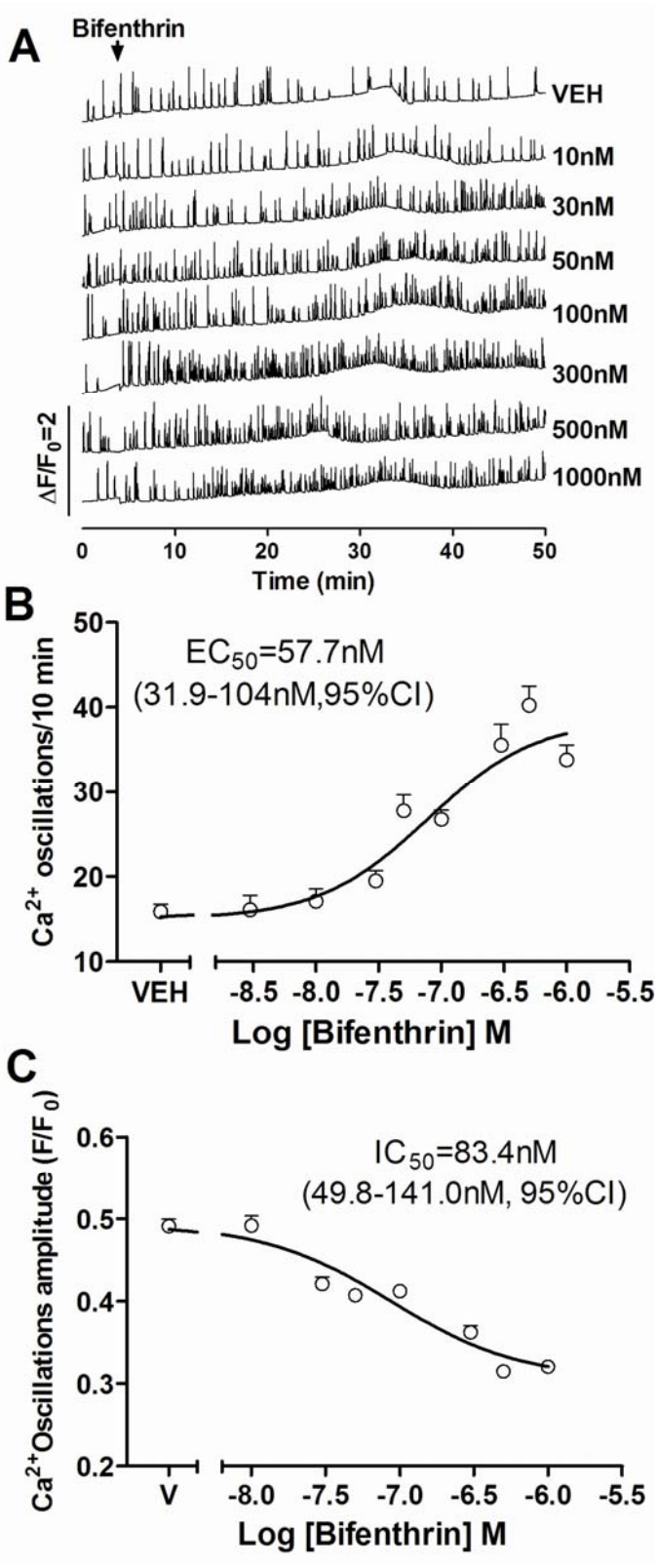

Figure 2

Molecular Pharmacology Fast Forward. Published on January 30, 2014 as DOI: 10.1124/mol.113.090076
This article has not been copyedited and formatted. The final version may differ from this version.

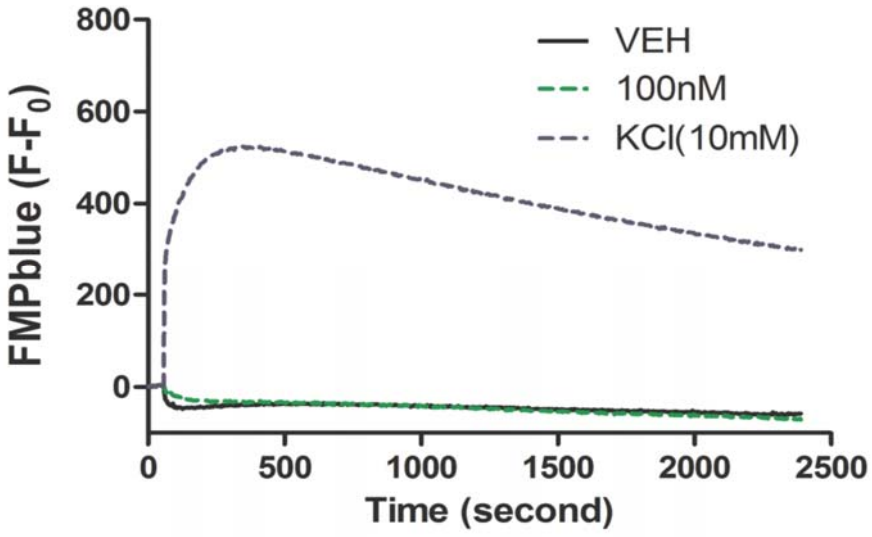

Figure 3

Molecular Pharmacology Fast Forward. Published on January 30, 2014 as DOI: 10.1124/mol.113.090076
This article has not been copyedited and formatted. The final version may differ from this version.

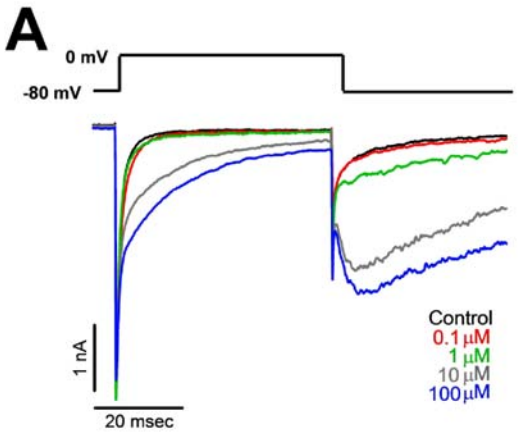

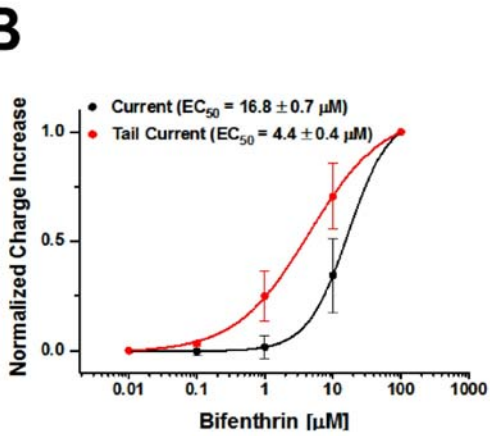

C

Bifenthrin [μM]	Current decay (msec)		Tail Current decay (msec)		n
	τ_1	τ_2	τ_1	τ_2	
DMSO control	0.4 ± 0.1	1.8 ± 0.7	0.9 ± 0.4	6.5 ± 1.0	3
0.1	0.5 ± 0.2	1.9 ± 1.0	0.9 ± 0.5	10.5 ± 1.8 (p = 0.029)	3
1	0.5 ± 0.2	2.7 ± 1.7	0.7 ± 0.4	12.9 ± 1.2 (p = 0.008)	3
10	0.4 ± 0.2	5.6 ± 0.9 (p = 0.005)	N.D.*	34.5 ± 16.4 (p = 0.042)	3
100	0.4 ± 0.1	8.1 ± 1.6 (p = 0.003)	N.D.*	62.0 ± 27.7 (p = 0.032)	3

* N.D. = Not determined. Tail current decay at these concentrations could not be fitted using a single exponential equation.

Figure 4

Molecular Pharmacology Fast Forward. Published on January 30, 2014 as DOI: 10.1124/mol.113.090076
This article has not been copyedited and formatted. The final version may differ from this version.

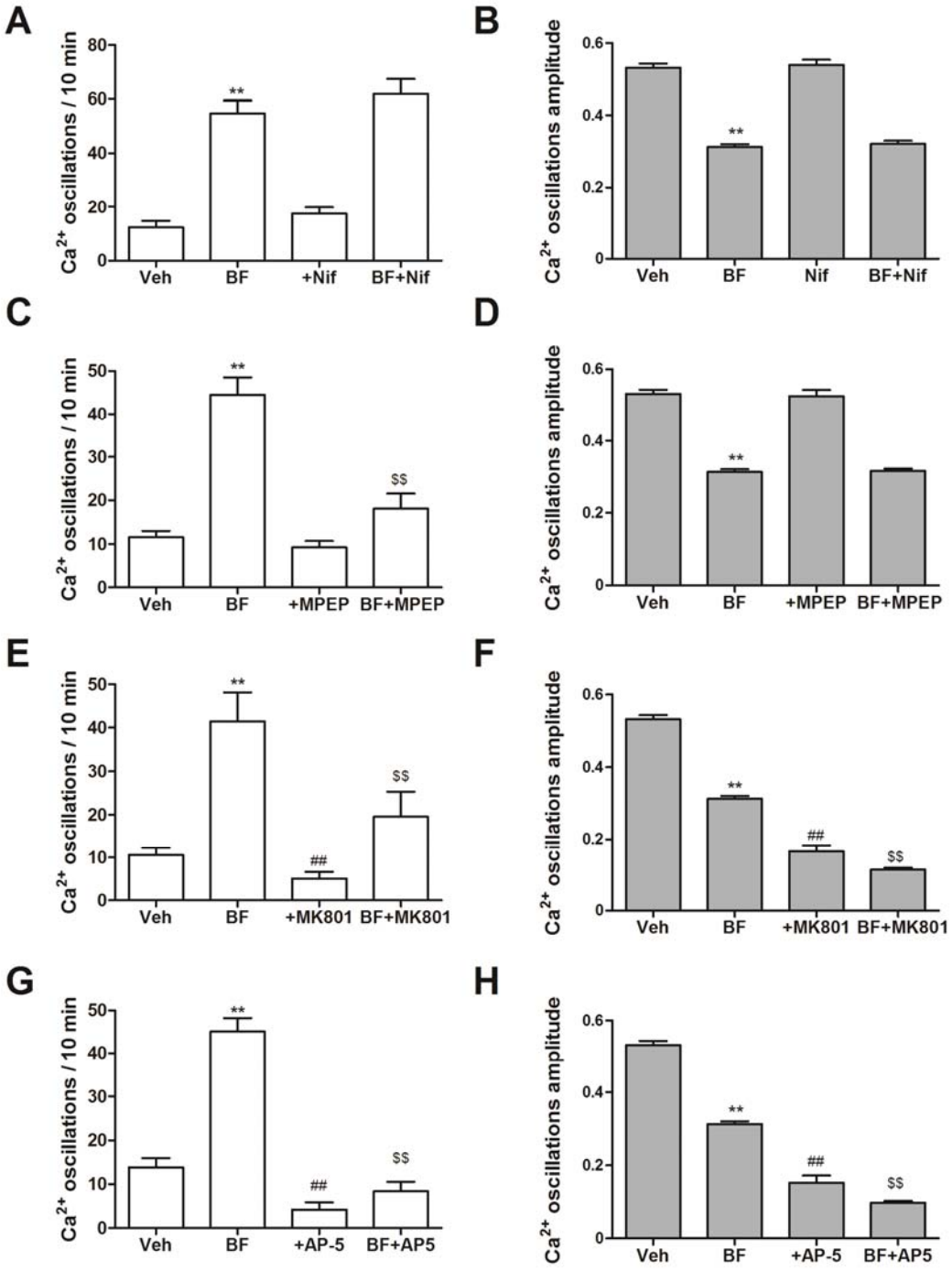

Figure 5

Molecular Pharmacology Fast Forward. Published on January 30, 2014 as DOI: 10.1124/mol.113.090076
This article has not been copyedited and formatted. The final version may differ from this version.

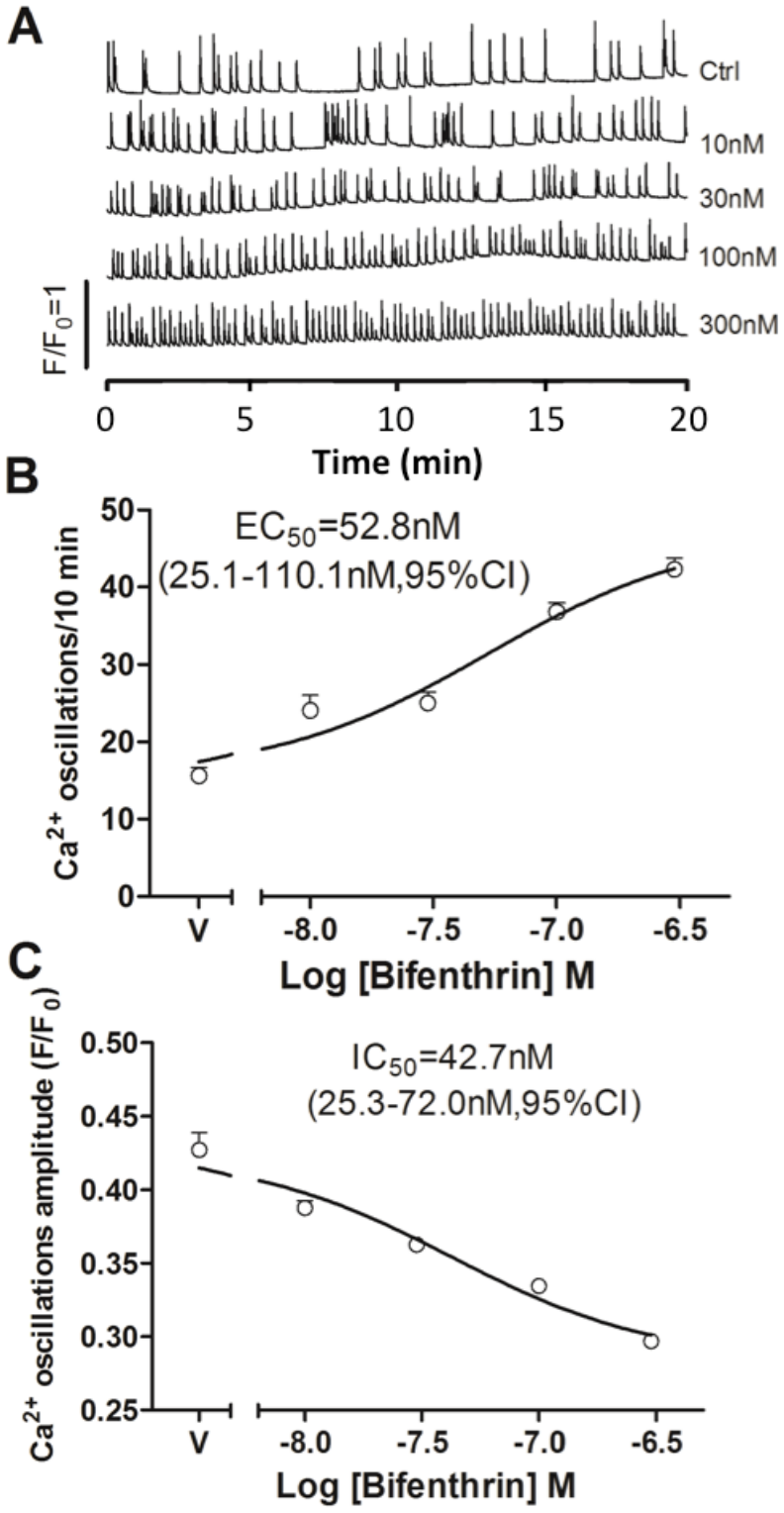

Figure 6

Molecular Pharmacology Fast Forward. Published on January 30, 2014 as DOI: 10.1124/mol.113.090076
This article has not been copyedited and formatted. The final version may differ from this version.

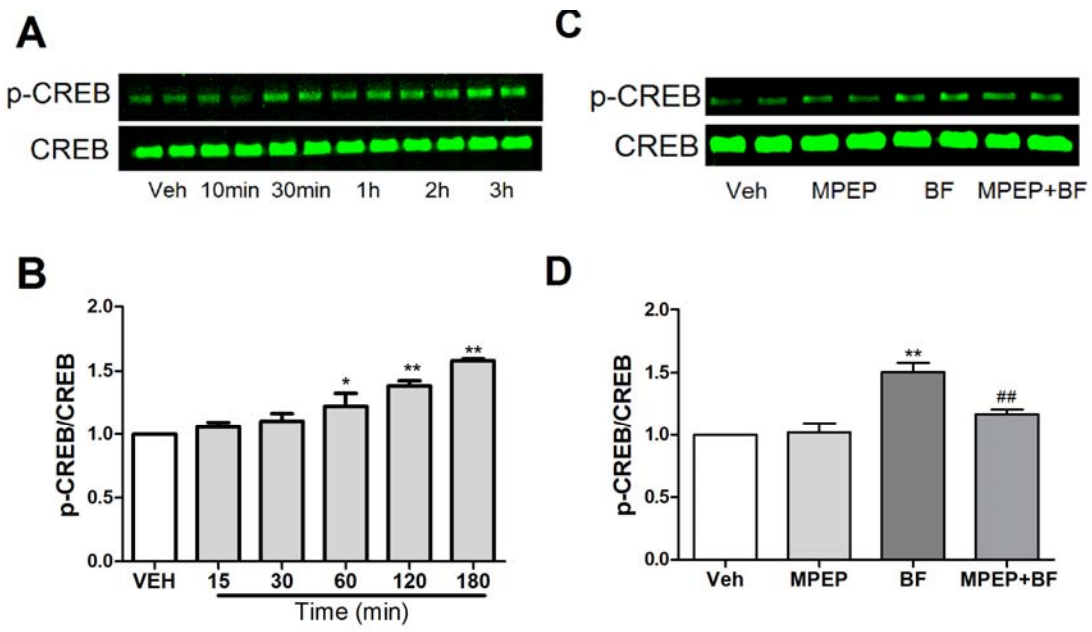

Figure 7

Molecular Pharmacology Fast Forward. Published on January 30, 2014 as DOI: 10.1124/mol.113.090076
This article has not been copyedited and formatted. The final version may differ from this version.

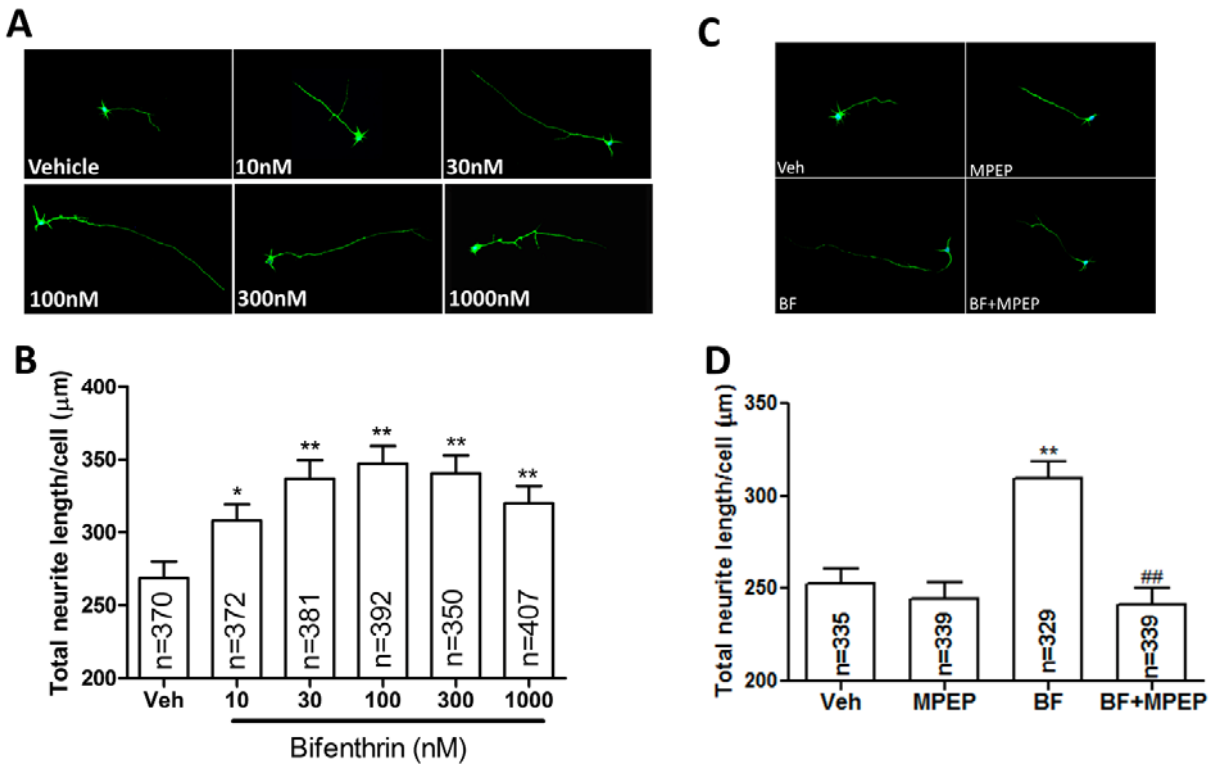

Figure 8

Nanomolar Bifenthrin Alters Synchronous Ca^{2+} Oscillations And Cortical Neuron Development Independent of Sodium Channel Activity

Zhengyu Cao, Yanjun Cui, Hai M. Nguyen, David Paul Jenkins, Heike Wulff, Isaac N. Pessah

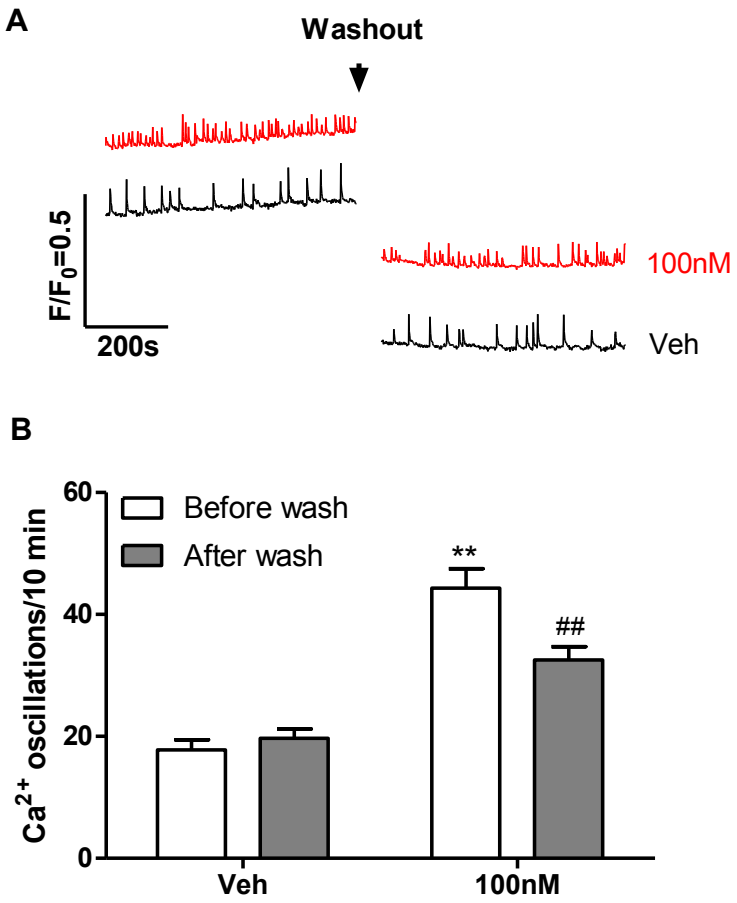

Supplementary Figure 1 | (A), Representative traces for spontaneous and bifenthrin-augmented Ca^{2+} oscillations before and after washout. (B), Quantification of bifenthrin-augmented Ca^{2+} oscillations frequency before and after complete wash for 5 times. Complete washout out of bifenthrin produces a partial recovery on the frequency of Ca^{2+} oscillations suggesting a persistent response on the spontaneous Ca^{2+} oscillations of bifenthrin. Each data point represents Mean±SEM (n=10) from two experiments each performed in quintuplicates.